Bioconjugate Chemistry

Article

pubs.acs.org/bc

Photophysical Properties and Synthesis of New Dye−Cyclooctyne Conjugates for Multicolor and Advanced Microscopy

Anna Hörner,[†,‡] Tobias Hagendorn,[†] Ute Schepers,*[,†,§] and Stefan Bräse*[,†,§]

[†]Institute of Organic Chemistry, Karlsruhe Institute of Technology, Fritz-Haber-Weg 6, 76131 Karlsruhe, Germany

[‡]Light Technology Institute, Karlsruhe Institute of Technology, Engesserstraße 13, 76131 Karlsruhe, Germany

[§]Institute of Toxicology and Genetics, Karlsruhe Institute of Technology, Hermann-von-Helmholtz-Platz 1, 76344 Eggenstein-Leopoldshafen, Germany

Supporting Information

ABSTRACT: Cyclooctyne conjugates with fluorophores are often used for bioorthogonal labeling in cells and tissues. However, no comprehensive library of one cyclooctyne core structure with different fluorescent dyes spanning the whole visible spectrum up to the NIR had been described so far. Hence, we synthesized and evaluated one cyclooctyne core structure which is easily accessible for the attachment of different dyes for multicolor imaging, FRET analysis, and study of metabolism in vivo. For these reasons we developed an easy one step synthesis starting from a known cyclooctyne. In combination with NHS-activated dyes, the cyclooctyne reacted to the dye DAB-MFCO conjugates within only 1−2 h at room temperature with high yields. We created conjugates with dyes that have high brightness and are bleaching stable with wavelengths from green to NIR. The ability to label glycans on cell surfaces was tested. All dye DAB-MFCO conjugates undergo click reactions on azide functionalized glycan structures with satisfactory photophysical properties. In total, seven different dye DAB-MFCO conjugates were synthesized; their photophysical properties and suitability for click labeling in biological applications were evaluated, making them suitable for single molecule and high resolution measurements.

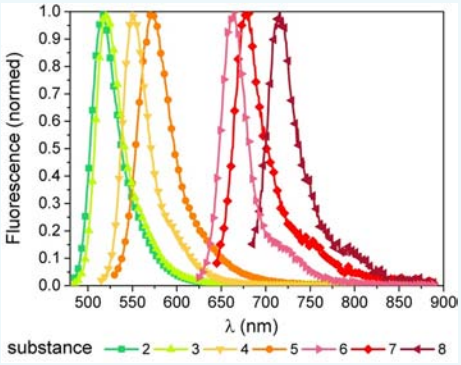

INTRODUCTION

Cyclooctynes are used in many fields as a versatile tool for labeling, e.g., as chemical reporters for DNA[1] and proteins[2] and also in material sciences.[3] They have become popular for bioorthogonal click labeling of glycan structures.[4] Glycans are important for cell−cell communication, recognition, adhesion, and interactions. They are also fundamental for the immune response, recognition of pathogens and other substances such as proteins, growth factors, signaling molecules, and drugs.[5,6] They are essential for cell differentiation during embryogenesis,[7] and many diseases with altered glycan structures are known.[8] Several of these recognition mechanisms are still unidentified as the glycome is not encoded by a genetic code; thus, it is generated by post-translational modifications. Until now, knowledge about glycan structures has been most commonly obtained by electron microscopy[9] or mass spectrometric analyses[10] of proteoglycans, glycoproteins, or glycolipids. To investigate interactions of those structures in space and time, they need to be visualized in vitro and in vivo, i.e., by labeling of glycan structures.

One of the first attempts to label glycan structures was carried out by Bertozzi and co-workers using the bioorthogonal Staudinger ligation after metabolizing azidosugar precursors.[11,12] It was shown that direct labeling of single sugars within the glycocalyx by a fluorophore could be achieved by bioorthogonal chemistry. Another approach to label glycan structures is by the use of CuAAC (Cu(I)-catalyzed azide−alkyne cycloaddition),[13−16] but this method is limited due to the use of free copper(I) because of its cell toxicity.

Bertozzi and co-workers were also the first ones to stain glycans on living cells with cyclooctynes by SPAAC (strain promoted azide−alkyne cycloaddition).[4] A couple of cyclooctynes were created for the use of SPAAC, for example, OCT,[4] DIBO,[17] BARAC,[18] COMBO,[19] DIFO,[20] BCN,[21,22] DIBAC,[23] and many more.[24−34] There are some procedures known for synthesis of dye−cyclooctyne conjugates with commercially available dyes.[18] However, the synthesis of those dye conjugates with the cyclooctynes mentioned above require rather laborious protocols. Furthermore, there is no comprehensive library of several dye conjugates with different fluorescent properties based on the same cyclooctyne core structure. Most of the conjugates therefore result in different reaction times for the click reaction. Here, we introduce a tool where many different dyes can be attached easily to one single core structure. The selected fluorophores were chosen due to their photophysical properties to create bleaching stable and bright dyes at a broad wavelength range. Due to the same click reaction conditions and the variety of different dyes, the conjugates are well suited for multicolor

Received: January 28, 2015
Revised: March 2, 2015
Published: March 3, 2015

DOI: 10.1021/acs.bioconjchem.5b00059
Bioconjugate Chem. 2015, 26, 718−724

imaging, here especially for single molecule detection and high resolution methods such as FCS, STED, STORM, and PALM.

RESULTS AND DISCUSSION

Synthesis. The fluorophore DAB-MFCO conjugates were designed based on their photophysical properties and the requested excitation wavelengths (Figure 1). For conjugation we

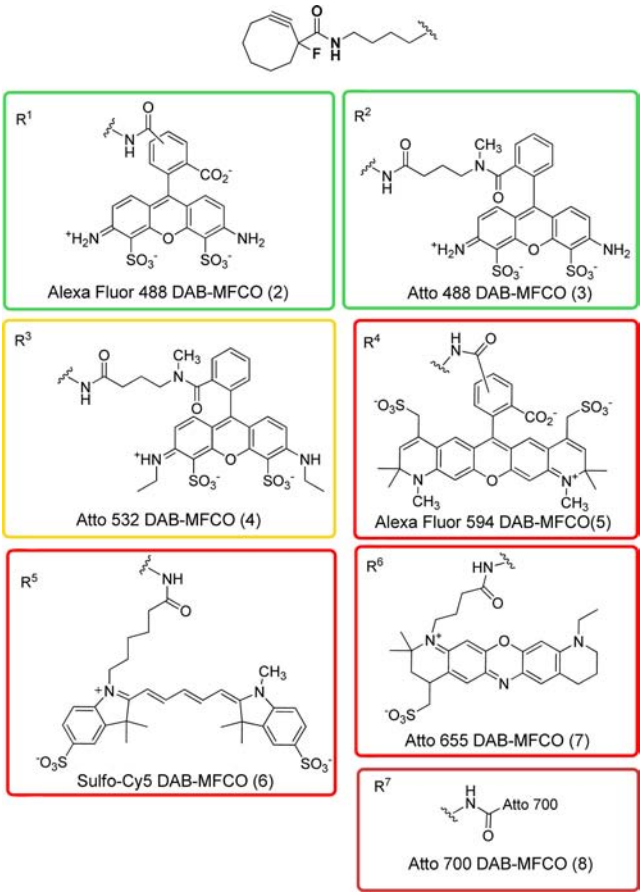

Figure 1. Chemical structures of the dye DAB-MFCO conjugates **2**–**8**.

used fluorophores with emission spectra within the whole visible wavelengths to near-infrared for multicolor labeling and in vivo measurements. Many of those dyes are known to be bleaching stable, which is essential for some microscopic techniques like photoactivated localization microscopy (PALM). The collection of a broad range of dyes now facilitates the choice of optimal conjugate pairs for multicolor imaging and FRET analysis.

The synthesis of the dye DAB-MFCO (diaminobutane monofluoro-substituted cyclooctyne) conjugates is straightforward (Scheme 1). The MFCO-amine **1** was prepared within five steps with a total yield of 27% from the commercially available methyl 2-oxocyclooctane-1-carboxylate.[35,36] The MFCO-amine **1** (10 equiv) was reacted with 1 equiv of the respective NHS-ester of the dye in 0.8 mL DMF for 1–2 h at room temperature. Afterward, the products **2**–**8** were directly purified by HPLC. The conversion was nearly quantitative for all fluorophores except compounds **2**, **4**, and **8**. Those components were reacted in less solvent and insoluble aggregates occurred. That lowered the yield to 79% for conjugate **2**, 89% for **4**, and 82% for compound **8**.

Scheme 1. Synthesis of the Dye DAB-MFCO Conjugates

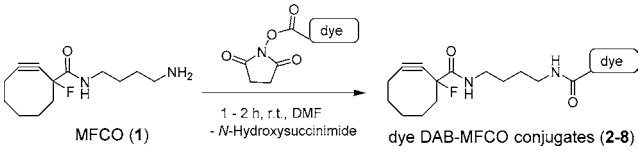

Spectroscopy. For most dye–cyclooctyne conjugates, photophysical properties have not been investigated so far. However, for many microscopic and spectroscopic measurements especially in the field of high resolution techniques, reagents with well validated photophysical properties are required. The photophysical properties of the dye DAB-MFCO conjugates were measured in phosphate buffer saline (PBS) at pH = 7.2 (Table 1, Figure 2, and Supporting Information). It was observed that the created dye DAB-MFCO conjugates cover the whole visible spectra up to NIR within a wavelength range from 494 to 702 nm. They also show fluorescence emission from 517 to 715 nm, respectively. They have Stokes shifts between 1 and 7 nm and quantum yields between 7% for the NIR conjugate **8** and 84% for Atto 488 DAB-MFCO (**3**) in the green region. Molar absorption coefficients (ε) vary between 0.9×10^4 and 8.2×10^4 M^{-1} cm^{-1} and the brightness of the conjugates is between 1.4×10^3 and 58.0×10^3 M^{-1} cm^{-1}. Thus, the conjugates show very good brightness for compounds **2**–**6** and medium brightness for the red-shifted compound **7** and the NIR conjugate **8**. To compare the brightness of the conjugates, the graduation goes from the brightest to the least bright conjugate from **3** (green), to **5** (red), to **6** (red), to **4** (yellow), to **2** (green), and to the NIR conjugates **8** and **7**.

After coupling of the NHS activated dye to the cyclooctyne (Table 1) photophysical properties for each dye changed. Absorption wavelengths show negligible changes for most of the conjugates. Absorption coefficients are unexceptional lower than those of the unconjugated dyes, but still appropriate for microscopic imaging. Emission shows slight bathochromic shifts from 2 nm and up to 7 nm for compound **7**. Only compound **6** does not show a bathochromic shift. Therefore, the Stokes shifts of the dye DAB-MFCO conjugates **2**–**5** and **7**–**8** are smaller in comparison with the unconjugated dyes. The presence of the diamine linker and the cyclooctyne allows for more degrees of freedom of vibration and rotation. Therefore, we expected the quantum yield to be lower for most of the conjugates. There is a strong influence of the quantum yield and the color of the dye DAB-MFCO conjugates. While the quantum yield remained unaltered for the green conjugate **3** with 84% ± 0.4%, it decreased to 82% for the green conjugate **2**, over 52% (**4**) for the yellow, to red 56% (**5**) and far red 26% (**6**), to 11% (**7**) and 7% (**8**) for the NIR-dyes. As a result, the brightness is lower for all measured dye DAB-MFCO conjugates compared to the unconjugated NHS-ester dyes. It varies from 5800 cm^{-1} M^{-1} for compound **3** to 140 cm^{-1} M^{-1} for the NIR conjugate **7**. From the photophysical data in Table 1 it is evident that the conjugation to the diamino-cyclooctyne moiety decreased the quantum yield for most dyes except dye **3**.

The DAB-MFCO conjugates were also measured in DMF, as they are mainly soluble in this solvent allowing for their application in standard organic reactions and solid phase synthesis (Table 2). The comparison of the photophysical properties of the dye DAB-MFCO conjugates in the two solvents reveals that most conjugates are red-shifted with the exception of the NIR conjugates. The most prominent shifts in the absorption

DOI: 10.1021/acs.bioconjchem.5b00059
Bioconjugate Chem. 2015, 26, 718–724

Table 1. Spectroscopic Values of Dye DAB-MFCO Conjugates and Their Unconjugated References in PBS pH 7.2[a].

	λ_{abs} (nm)			λ_{em} (nm)			Stokes shift			molar absorption coefficient $\varepsilon \times 10^4$ ($M^{-1}cm^{-1}$)			quantum yield Φ			brightness $H \times 10^4$ (M^{-1} cm^{-1})		
compound	ref dye	dye-CO	Δ	ref dye	dye-CO	Δ	ref dye	dye-CO	Δ	ref dye	dye-CO	CO/ref.	ref dye	dye-CO	CO/ref.	ref dye	dye-CO	CO/ref.
2	495	494	−1	519	517	−2	24	23	−1	7.1	0.9	0.13	0.92	0.82	0.89	6.53	0.74	0.11
3	501	502	1	523	521	−2	22	19	−3	9.0	6.9	0.77	0.80	0.84	1.05	7.20	5.80	0.81
4	532	533	1	551	550	−1	21	17	−4	11.5	2.6	0.23	0.90	0.52	0.58	10.35	1.35	0.13
5	590	587	−3	617	612	−5	27	25	−2	9.0	4.4	0.49	0.66	0.56	0.85	5.94	2.46	0.41
6	646	646	0	662	663	1	16	17	1	27.1	8.2	0.30	0.27[37]	0.26	0.96	7.32	2.13	0.29
7	663	663	0	684	677	−7	21	14	−7	12.5	1.3	0.10	0.30	0.11	0.37	3.75	0.14	0.04
8	700	702	2	719	715	−3	19	13	−6	12.0	4.0	0.33	0.25	0.07	0.28	3.00	0.28	0.09

[a]ref. dye = the according uncoupled dye provided by the supplying companies; dye-CO = dye DAB-MFCO conjugate. For data, including deviations, see Supporting Information.

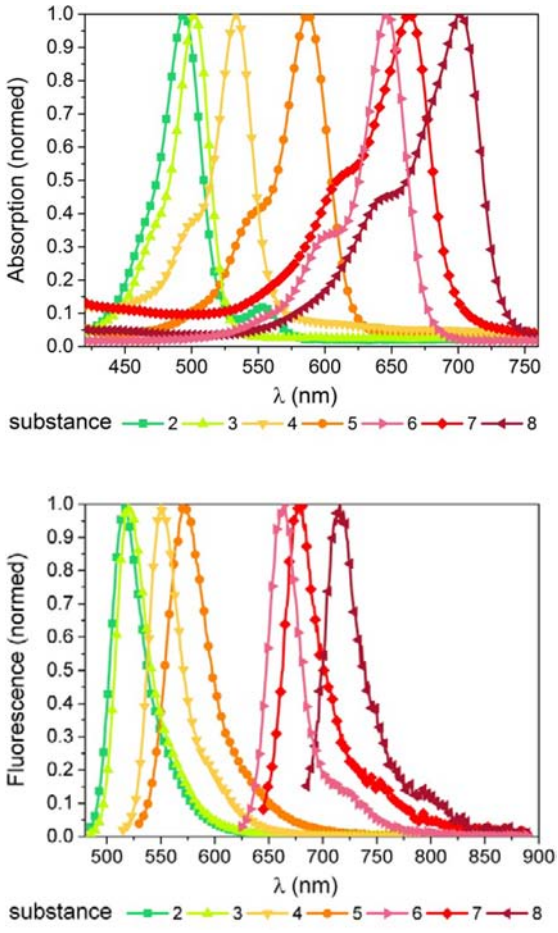

Figure 2. Absorption and emission spectra in PBS; from left to right: green = Alexa 488 DAB-MFCO (**2**), light green = Atto 488 DAB-MFCO (**3**), orange = Atto 532 DAB-MFCO (**4**), dark orange = Alexa 594 DAB-MFCO (**5**), light red = Sulfo-Cy5 DAB-MFCO (**6**), red = Atto 655 DAB-MFCO (**7**), dark red = Atto 700 DAB-MFCO (**8**).

spectra are for conjugates **2** and **3** with 74 nm for conjugate **2** and 13 nm for conjugate **3**. The emission is also bathochromically shifted for conjugates **2**−**6** with 9 nm for conjugate **5** to 64 nm for conjugate **2**. The comparison of the molar absorption coefficient reveals that the order of magnitude is similar in both solvents for the same compound with exception of conjugates **2** and **5**.

Furthermore, it is notable that values for the quantum yield and brightness are higher for most dye DAB-MFCO conjugates in DMF with exception of compounds **2** and **5**. Comparing the brightness for compound **2** (H = 30 M^{-1} cm^{-1} in DMF and 740 M^{-1} cm^{-1} in PBS) and **5** (H = 50 M^{-1} cm^{-1} in DMF and 2460 M^{-1} cm^{-1} in PBS), the effect is more than 1 order of magnitude higher in PBS for **5**; the effect is even stronger than for **2**. Those two conjugates carry Alexa Fluor dyes bearing a carboxylate group on the phenyl ring, while the others do not. It is reasonable that the negative charge is better stabilized in the PBS buffer and destabilized in DMF, and therefore the values are higher in PBS than in DMF.

For all other substances, the values are higher in DMF compared to PBS. (For data, including deviations, see Supporting Information.)

Lifetime Measurements. As described above, this comprehensive library of different dye DAB-MFCO conjugates facilitate selection of appropriate FRET pairs. The conjugates can be used as FRET pairs not only for spectroscopy and microscopy, but also for combined methods such as lifetime imaging and FRET-interactions. The lifetimes of the dye DAB-MFCO conjugates were evaluated in PBS. Table 3 shows lifetimes between 1.24 ns for compound **6** and 4.89 ns for conjugate **5**. For all dye DAB-MFCOs the lifetime values increased compared to the NHS-ester activated dyes, except for the NIR conjugate **7**.

Due to the same click reaction conditions and kinetics and the variety of different dyes, the conjugates are well suited for a variety of applications such as multicolor imaging, and especially for single molecule detection and high resolution methods such as FCS, STED, STORM, and PALM, as well as for FRET, in vivo imaging, and surface modifications (Table 4). The high resolution technologies enable the resolution down to 10 nm with dyes comprising superior photophysical criteria. Some Atto-dyes such as Atto 488 and Atto 655 have proven suitable for those techniques.

Bioorthogonal Labeling in HeLa Cells. To show their suitability for biorthogonal labeling of cells, glycostructures on cell surfaces were labeled using the dye DAB-MFCO conjugates **2**−**8**. 1 × 10^4 HeLa cells were incubated for 3 days with 80 μM Ac_4ManNAz to allow metabolization into cell surface glycostructures. Eventually, 20 μM of the respective dye DAB-MFCO **2**−**8** was added and incubated for 4 h at 37 °C to start the SPAAC. After counterstaining of the nuclei with Hoechst 33342 the cells were subjected to confocal fluorescent microscopy (Figure 3). This experiment shows clear fluorescent labeling of the plasmamembrane glycostructures and the suitability of the novel dye-cyclooctynes for click reaction with azides. They also show endosomal accumulation, which is mainly due to the endocytosis of the labeled glycostructures.

DOI: 10.1021/acs.bioconjchem.5b00059
Bioconjugate Chem. 2015, 26, 718−724

Table 2. Spectroscopic Values of the Dye DAB-MFCO Conjugates in PBS pH 7.2 Compared to DMF[a]

	λ_{abs} (nm)			λ_{em} (nm)			Stokes shift			molar absorption coefficient $\varepsilon \times 10^4$ (M^{-1} cm^{-1})			quantum yield Φ			$H \times 10^4$ (M^{-1} cm^{-1})		
compound	in DMF	in PBS	Δ	in DMF	in PBS	Δ	in DMF	in PBS	Δ	in DMF	in PBS	PBS/DMF	in DMF	in PBS	PBS/DMF	in DMF	in PBS	PBS/DMF
2	568	494	−74	581	517	−64	13	23	10	0.1	0.9	9.00	0.32	0.82	2.56	0.03	0.74	23.06
3	515	502	−13	533	521	−12	18	19	1	8.0	6.9	0.86	0.80	0.84	1.05	6.42	5.80	0.90
4	542	533	−9	560	550	−10	18	17	−1	2.1	2.6	1.21	0.89	0.52	0.58	1.90	1.35	0.71
5	595	587	−8	621	612	−9	26	25	−1	0.3	4.4	14.67	0.16	0.56	3.50	0.05	2.46	51.33
6	657	646	−11	677	663	−14	20	17	−3	8.0	8.2	1.03	0.51	0.26	0.51	4.08	2.13	0.52
7	662	663	1	675	677	2	13	14	1	1.7	1.3	0.79	0.46	0.11	0.24	0.76	0.14	0.18
8	699	702	3	715	715	0	16	13	−3	5.7	4.0	0.70	0.52	0.07	0.13	2.96	0.28	0.09

[a]For data, including deviations, see Supporting Information.

Table 3. Lifetime Measurements of the Conjugates in PBS pH 7.2[a]

compound	τ [ns] dye-DAB-MFCO in PBS	τ [ns] reference in PBS	τ [ns] dye-DAB-MFCO in water	τ [ns] reference in water
2	4.35 ± 0.13	-	4.42 ± 0.03	4.1[38]
3	4.60 ± 0.11	4.1	4.66 ± 0.03	4.1[39]
4	4.34 ± 1.65 × 10^{-15}	3.8	-	3.8[39]
5	4.89 ± 0.82	-	4.28 ± 0.05	3.9[38]
6	1.24 ± 0.03	1.0[40]	-	
7	2.35 ± 0.06	4.0	-	1.8[39]

[a]Reference = uncoupled dye provided by the manufacturer.

Table 4. Applications for the Various DAB-MFCOs

application	compounds	ref
bioconjugation	**2**, **3**, **4**, **5**, **6**, **7**, **8**	
fluorescence microscopy	**2**, **3**, **4**, **5**, **6**, **7**, **8**	
confocal microscopy	**2**, **3**, **4**, **5**, **6**, **7**, **8**	
dual color labeling	**2**, **3**, or **4** and **5**, **6**, **7**, or **8**	
	5 and **6**, **7**, or **8**	
triple color labeling	**2**, **3**, or **4** and **5** and **6**, **7**, or **8**	
in vivo imaging	**7**, **8**	
FRET pairs	(**2**, **3**/**4**, **5**, **6**, **7**) (**5**/**6**, **7**, **8**) (**4**/**5**, **6**, **7**, **8**) (**6**/**7**, **8**) (**7**/ **8**)	
STED	**2**[a], **4**[a], **5**[b], **7**	41−43
dual color STED	**5** and **7**	
TIRF	**2**, **3**, **6**	42
FCS spectroscopy	**2**, **3**, **4**, **5**, **6**, **7**	
PALM	**3** and **6**	42,43
STORM	**6**	42,47
dual color STORM	**3** and **6**	47
nRI Western blot	**8**	
surface labeling	(**2**), **3**, **4**, **5**, (**6**), **7**, **8**	44
microarray application	**3**, **4**, **7**	
materials	**2**, **3**, **4**, **5**, **6**, **7**, **8**	45

[a]STED Laser 660 nm. [b]STED special conditions: STED laser 660 nm better than 775 nm.

The reaction time for the SPAAC is chosen between 2 and 4 h as this is a compromise between the strength of the labeling at the plasmamembrane and the rate of endocytic internalization (see Supporting Information). Although there are other cyclooctynes with much faster kinetics, this cyclooctyne core is easily accessible and allows for many different labeling reactions and costaining, e.g., colocalization studies.

It is also visible in Figure 3 that the dye DAB-MFCO conjugates are able to undergo endocytosis and enter into the cells by themselves; this effect is shown to take place after longer incubation times. This means that the conjugates themselves are able to enter the living cells without further cell culture treatment and azides inside the cells can be labeled likewise, e.g., alkynes in endosomes, lysosomes, and other cell compartments.

CONCLUSION

A small comprehensive library of seven dye DAB-MFCO conjugates were prepared by an easy synthesis, analyzed with spectroscopic methods, and tested for their application in bioorthogonal labeling in cells. The synthesis is straightforward and can be done in one step from MFCO **1** to the dye DAB-MFCO conjugates with high yields. Various dye DAB-MFCO conjugates were synthesized covering the whole visible spectra to NIR for excitation and emission wavelengths. They show high molar absorption coefficients, high quantum yields, and good brightness depending on the wavelengths of the conjugates. The far-red and NIR conjugates are lower in quantum yield and brightness than the conjugates in the visible region, especially green and red. This shows that the addition of the DAB-MFCO moiety has more influence on the far-red to NIR than to shorter-wavelength conjugates. Also, lifetimes of the fluorophores were measured and show clear fluorescence behavior in PBS with τ = 1.24−4.66 ns. Measurements of the DAB-MFCO conjugates in DMF show a strong red shift of nearly all conjugates and also higher quantum yields and brightness with the exception of conjugates **2** and **5**. All dye DAB-MFCO conjugates show labeling of cell surface glycan structures with biorthogonal click reactions. Also, the conjugates show internalization into the cells without further cell culture treatment; therefore, the conjugates can also be used to stain cell compartments, like endosomes and other azido functionalized structures inside the cell.

METHODS

Solvents and chemicals used were purchased from Sigma-Aldrich, Taufkirchen, Germany; Atto-Tec, Siegen, Germany; Life technologies, Darmstadt, Germany; and Lumiprobe, Hallandale Beach, USA. Purification of the conjugates were done by reversed phase preparative HPLC using a JASCO HPLC system, using a RPC18 protein and peptide column (Grace Davison Discovery Sciences, 10 μm, 22 × 250 mm). Flow rate: 15 mL/min with gradient of A: 5% acetonitrile in water (+ 0.1% TFA) to B: 95% acetonitrile in water (+ 0.1% TFA). The purity was determined at the excitation wavelength of the substances. HRMS (high resolution mass spectrometry) were carried out on a Mascom

DOI: 10.1021/acs.bioconjchem.5b00059
Bioconjugate Chem. 2015, 26, 718−724

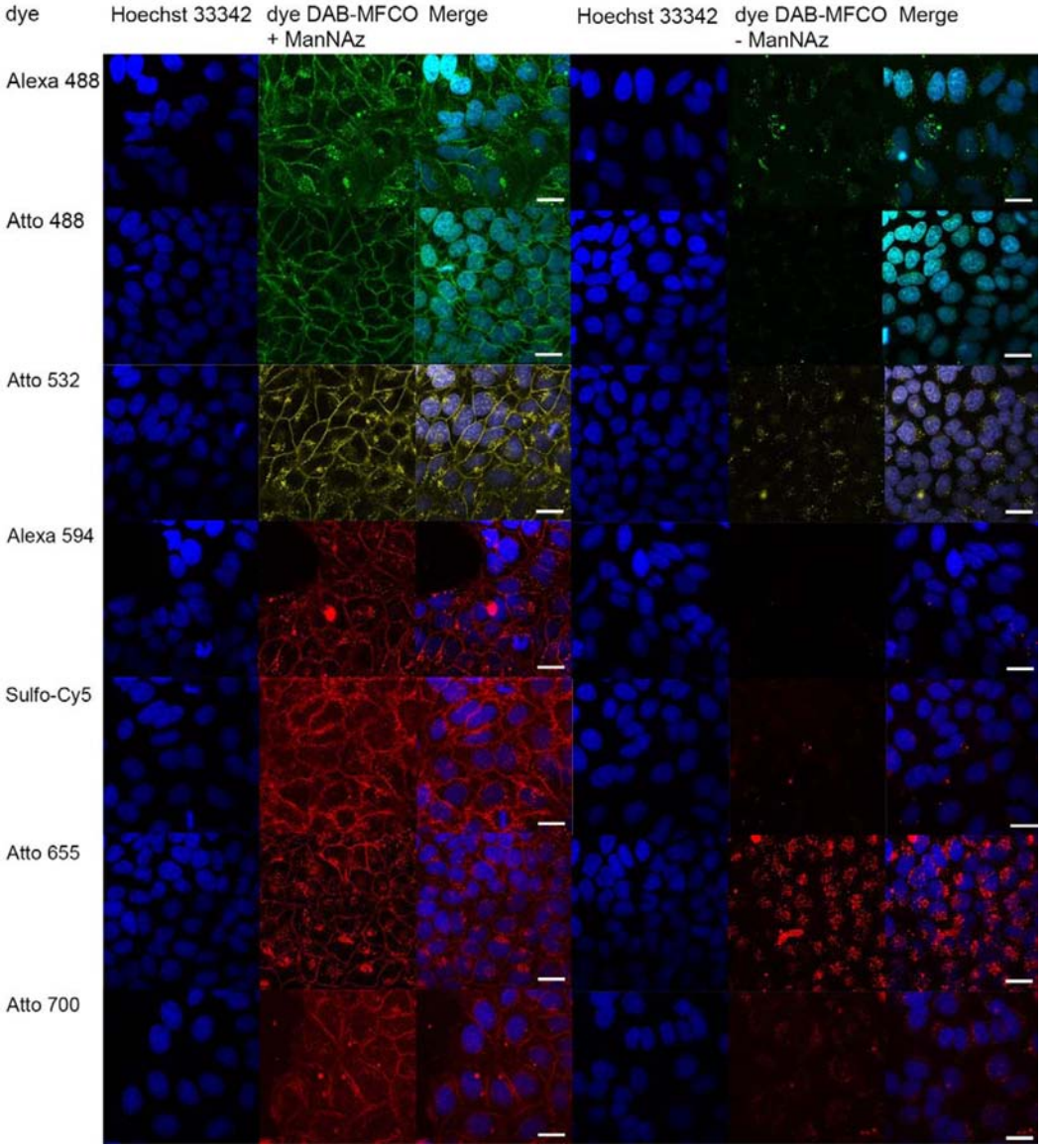

Figure 3. 1×10^4 HeLa cells/well were incubated in IBItreat 8 μ-well chamber slides with 80 μM Ac_4ManNAz (+ ManNAz, three columns on the left side) or without Ac_4ManNAz (− ManNAz, three columns on the right side) in DMEM for 3 days at 37 °C and 5% CO_2. Eventually, the cells were incubated with 20 μM of dye DAB-MFCO in DMEM for 4 h at 37 °C and 5% CO_2, and the nuclei were counterstained with 0.5 μg/mL Hoechst 33342 for 15 min. Images were taken by using a Leica SP5-TCS (DMI6000) inverse microscope. The laser power used was 30% of the argon laser with the emissive wavelengths 488 and 514 nm. A HeNe Laser was used for the wavelengths 594 and 633 nm with an additional UV DIOD for 351 and 364 nm. Objective: HCX PL APO CS 63.0 × 1.20 WATER UV. Hoechst33342 had been excited with λ_{ex} = 364 nm, Alexa 488 DAB-CO (**2**) and Atto 488 DAB-CO (**3**) with λ_{ex} = 488 nm, Atto 532 DAB-CO (**4**) with λ_{ex} = 514 nm, Alexa 594 DAB-CO (**5**) with λ_{ex} = 594 nm, Sulfo-Cy5 DAB-CO (**6**) with λ_{ex} = 561 nm, Atto 655 DAB-CO (**7**) and Atto 700 DAB-CO (**8**) with λ_{ex} = 633 nm. Scale bar 20 μm. (For further information, see Supporting Information).

MAT 95. Descriptions without nominated temperature were done at room temperature (r.t.), and the following abbreviations were used: calcd. (theoretical value), found (measured value).

Photophysical Measurements. Absorption and emission spectra of the dye DAB-MFCO conjugates **2**−**8** were measured in PBS pH 7.2 and DMF (HPLC grade). Absorption measurements were done on a Cary 300 UV Visible Spectrometer, Varian, Agilent Technologies. Fluorescence spectra were recorded on a Cary Eclipse Fluorescence Spectrophotometer, Varian, Agilent Technologies. Quantum yields were determined in solution calculated by the reference method.[46] As standard, 5,6-carboxyfluorescein was used for compounds **2** and **3**, Atto 532-NHS for compound **4**, Rhodamine 6G for compound **5**, Sulfo-Cy5-NHS for compounds **6** and **7**, and Alexa 700-NHS for compound **8**. Fluorescence lifetime measurements were recorded with a Horiba Scientific FluoroMax-4 spectrofluorometer using a JX monochromator and detected using the TCSPC method with the FM-2013 accessory and a TDSPC hub from Horiba Yvon Jobin. A NanoLED 370 nm, 1.5 ns pulse was used as excitation source. Decay curves were analyzed with the software DAS-6 and DataStation provide by Horiba Yvon Jobin. The quality of the fit was determined by the χ^2 method by Pearson.

Cell Culture and Treatment. Human cervix carcinoma cells (HeLa cells) were cultured in Dulbecco's modified Eagle medium (DMEM) supplemented with 10% fetal calf serum and 1% penicillin streptomycin (100 μg/mL) at 37 °C and 5% CO_2. For imaging experiments, 1×10^4 HeLa cells per well were

DOI: 10.1021/acs.bioconjchem.5b00059
Bioconjugate Chem. 2015, 26, 718−724

seeded in an 8-well chamber slide (μ Slide 8 well ibiTreat, IBIDI) in 200 μL of media. The cells were incubated with 80 μM Ac_4ManNAz for 3 days at 37 °C, 5% CO_2. Eventually, they were washed 3 times with media and incubated with 20 μM of the respective dye DAB-MFCO conjugate for 1−4 h. Afterward, they were washed 3 times and incubated with 0.5 μg/mL Hoechst 33342 for 15 min.

Confocal Microscopy. Cell images showing the fluorescence were obtained by confocal fluorescence microscopy using a Leica SP5 −TCS DM(I)6000 inverted microscope, a HCX PL APO CS63.0 × 1.20 WATER UV objective. Imaging was performed according to the settings as described in the Results section.

Synthesis. For some of the dye-NHS esters no exact structure including anions is available. In these cases the molecular weight and thus the yields were calculated based on the MW provided by the manufacturer by substituting the NHS-group with the attached cyclooctyne moiety. One milligram amounts were weighed and given by the suppliers.

Alexa Fluor 488 DAB-MFCO ***2***. Alexa Fluor 488-NHS ester (1 mg, 1.55 μmol, 1 equiv) and 3.7 mg of the MFCO-amine (**1**) (15.3 μmol, 10 equiv) were reacted in 30 μL DMF for 1 h by shaking. The conjugate was purified by HPLC yielding 0.94 mg of **2** (79%, 1.22 μmol according to M(M^+A^-) 768.64 g/mol) as an orange-red powder. Analytical HPLC (5−95% acetonitrile within 30 min): t_{ret} = 12.3 min. HR-FAB ($C_{34}H_{29}FN_4O_{11}S_2Li_3^+$): calcd. 773.1733; found 773.1734.

Atto 488 DAB-MFCO ***3***. Atto 488-NHS ester (anion unknown, 1 mg, 1.02 μmol, 1 equiv) and 2.4 mg of the MFCO-amine (**1**) (9.99 μmol, 10 equiv) were reacted in 400 μL DMF for 2 h by shaking. Afterward, the conjugate was purified by HPLC yielding 1.13 mg of conjugate **3** (according to the calculated M(M^+A^-) 1107 g/mol) as an orange-red powder. As the counterion is not known the correct yield cannot be calculated. Analytical HPLC (5−95% acetonitrile within 30 min): t_{ret} = 10.4 min. − HR-FAB ($C_{38}H_{42}FN_5O_{10}S_2Na^+$): calcd. 834.2249; found 834.2245.

Atto 532 DAB-MFCO ***4***. Atto 532-ester (anion unknown, 1 mg, 0.925 μmol, 1 equiv) and the MFCO-amine (**1**) (2.2 mg, 9.170 μmol, 10 equiv) were reacted in 30 μL DMF for 1 h by shaking. Afterward, the conjugate was purified by HPLC yielding 0.99 mg of **4** (89%, 0.821 μmol M(M^+A^-) 1206 g/mol) as a deep pink solid. Analytical HPLC (5−95% acetonitrile within 30 min): t_{ret} = 12.3 min. HR-FAB ($C_{42}H_{50}FN_5O_{10}S_2Na^+$): calcd. 890.2875; found 890.2869.

Alexa Fluor 594 DAB-MFCO ***5***. Alexa Fluor 594-NHS ester (1 mg, 1.21 μmol, 1 equiv) and the MFCO-amine (**1**) (2.9 mg, 12 μmol, 10 equiv) were reacted in 400 μL DMF for 2 h by shaking. Afterward, the conjugate was purified by HPLC yielding 1.14 mg of **5** (according to M(M^+A^-) 945.3 g/mol) as a blue powder. As analytical HPLC of the purified product showed several peaks and mass spectrometry of submilligram amounts of the analytical fractions was not feasible, the overall yield could not be determined. Analytical HPLC (5−95% acetonitrile within 30 min): t_{ret} = 9.7−11.7 min. HR-FAB ($C_{48}H_{54}FN_4O_{11}S_2^+$): calcd. 945.3209; found 945.3204.

Sulfo-Cy5 DAB-MFCO ***6***. Sulfo-Cy5-NHS-ester (1 mg, 1.31 μmol, 1 equiv) and 3.1 mg of the MFCO-amine (**1**) (12.9 μmol, 10 equiv) were reacted in 800 μL DMF for 2 h by shaking. Afterward, the conjugate was purified by HPLC yielding 1.13 mg of **6** (97%, 1.27 μmol according to M(M^+A^-) 887 g/mol) as a blue powder. Analytical HPLC (5−95% acetonitrile within 30 min): t_{ret} = 10.0 min. HR-FAB ($C_{45}H_{58}FN_4O_8S^{2+}$): calcd. 865.3675; found 865.3678.

Atto 655 DAB-MFCO ***7***. Atto 655-NHS ester (1 mg, 1.13 μmol, 1 equiv) and the MFCO-amine (**1**) (3.8 mg, 16.0 μmol, 14 equiv) were reacted in 500 μL DMF for 1 h by shaking. Afterward, the conjugate was purified by HPLC yielding 1.15 mg of the desired compound **7** (according to M(M^+A^-) 1012 g/mol) as a blue-green solid. As analytical HPLC of the purified product showed several peaks and mass spectrometry of submilligram amounts of the analytical fractions was not feasible, the overall yield could not be determined. Analytical HPLC (5−95% acetonitrile within 30 min): t_{ret} = 17.6 min. HR-FAB ($C_{40}H_{53}FN_5O_6S^+$): calcd. 750.3695; found 750.3693.

Atto 700 DAB-MFCO ***8***. Atto 700-NHS ester (1 mg, 1.19 μmol, 1 equiv) and the MFCO-amine (**1**) (2.8 mg, 11.67 μM, 10 equiv) were reacted in 400 μL DMF for 2 h, by shaking. Afterward, the conjugate was purified by HPLC and 0.94 mg of **8** (82%, 0.98 μmol according to M(M^+A^-) 962 g/mol) was obtained as a blue-green solid. Analytical HPLC (5−95% acetonitrile within 30 min): t_{ret} = 14.5 min. HR-FAB (structure not known, due to patent pending; mass provided by the company): calcd. 786.86 ± 1; found 787.2.

■ ASSOCIATED CONTENT

Supporting Information

Preparative and analytical HPLC traces of the conjugates, mass spectra, and detailed spectroscopic values. This material is available free of charge via the Internet at http://pubs.acs.org.

■ AUTHOR INFORMATION

Corresponding Authors

*E-mail: ute.schepers@kit.edu. Phone: +49721 608-23444. Fax: +49 721 608-23354.

*E-mail: Braese@kit.edu. Phone: +49721 608-42902. Fax: +49 721 608-48581.

Author Contributions

All authors have given approval to the final version of the manuscript.

Notes

The authors declare no competing financial interest.

■ ACKNOWLEDGMENTS

We want to thank the Carl-Zeiss-Stiftung (AH), Karlsruhe School of Optics and Photonics (KSOP) (AH), and the Landesgraduiertenförderung Baden-Württemberg (TH) for financial support. Further, we want to thank Daniel Volz and the Cynora GmbH for help with the lifetime measurements. The work was funded by the Helmholtz Program Biointerface and the DFG research group GRK2039.

■ ABBREVIATIONS

BARAC, biarylazacyclooctynone; BCN, bicycle[6.1.0] nonyne; COMBO, carboxymethylmonobenzocyclooctyne; CO, cyclooctyne; DAB-MFCO, diaminobutane−monofluoro-substituted cyclooctyne; DIBAC, dibenzo-aza-cyclooctyne; DIBO, dibenzocyclooctyne; DIFO, difluorinated cyclooctyne; DMF, dimethylformamide; ε, molar absorption coefficient; FRET, Förster resonance energy transfer; equiv, equivalents; H, brightness; HPLC, high-performance liquid chromatography; MFCO, monofluoro-substituted cyclooctyne; NHS, *N*-hydroxysuccinimide; NIR, near-infrared; PBS, phosphate buffer saline; Φ, quantum yield

DOI: 10.1021/acs.bioconjchem.5b00059
Bioconjugate Chem. 2015, 26, 718−724

REFERENCES

(1) Singh, I., and Heaney, F. (2011) *Chem. Commun. 47*, 2706−8.
(2) Wammes, A. E. M., Fischer, M. J. E., de Mol, N. J., van Eldijk, M. B., Rutjes, F. P., van Hest, J. C. M., and van Delft, F. L. (2013) *Lab Chip 13*, 1863−7.
(3) Wang, Z., Liu, J., Arslan, H. K., Grosjean, S., Hagendorn, T., Gliemann, H., Bräse, S., and Wöll, C. (2013) *Langmuir 29*, 15958−64.
(4) Agard, N. J., Prescher, J. A., and Bertozzi, C. R. (2004) *J. Am. Chem. Soc. 126*, 15046−15047.
(5) Hakomori Si, S. I. (2002) *Proc. Natl. Acad. Sci. U. S. A. 99*, 225−32.
(6) Becker, B. F., Chappell, D., Bruegger, D., Annecke, T., and Jacob, M. (2010) *Cardiovasc. Res. 87*, 300−10.
(7) Becker, D. J., and Lowe, J. B. (2003) *Glycobiology 13*, 41R−53R.
(8) Praissman, J. L., and Wells, L. (2014) *Biochemistry 53*, 3066−78.
(9) Chappell, D., Jacob, M., Paul, O., Rehm, M., Welsch, U., Stoeckelhuber, M., Conzen, P., and Becker, B. F. (2009) *Circ. Res. 104*, 1313−7.
(10) Cao, L., Zhang, Y., Chen, L., Shen, A., Zhang, X., Ren, S., Gu, J., Yu, L., and Liang, X. (2014) *Analyst 139*, 4538−46.
(11) Saxon, E., and Bertozzi, C. R. (2000) *Science 287*, 2007−10.
(12) Schilling, C. I., Jung, N., Biskup, M., Schepers, U., and Bräse, S. (2011) *Chem. Soc. Rev. 40*, 4840−71.
(13) Tornøe, C. W., Christensen, C., and Meldal, M. (2002) *J. Org. Chem. 67*, 3057−3064.
(14) Rostovtsev, V. V., Green, L. G., Fokin, V. V., and Sharpless, K. B. (2002) *Angew. Chem., Int. Ed. 41*, 2596−2599.
(15) Bräse, S., Gil, C., Knepper, K., and Zimmermann, V. (2005) *Angew. Chem., Int. Ed. 44*, 5188−240.
(16) Kölmel, D. K., Jung, N., and Bräse, S. (2014) *Aust. J. Chem. 67*, 328−336.
(17) Ning, X., Guo, J., Wolfert, M. A., and Boons, G. J. (2008) *Angew. Chem., Int. Ed. 47*, 2253−5.
(18) Jewett, J. C., Sletten, E. M., and Bertozzi, C. R. (2010) *J. Am. Chem. Soc. 132*, 3688−3690.
(19) Varga, B. R., Kallay, M., Hegyi, K., Beni, S., and Kele, P. (2012) *Chemistry 18*, 822−8.
(20) Codelli, J. A., Baskin, J. M., Agard, N. J., and Bertozzi, C. R. (2008) *J. Am. Chem. Soc. 130*, 11486−11493.
(21) Dommerholt, J., Schmidt, S., Temming, R., Hendriks, L. J. A., Rutjes, F. P. J. T., van Hest, J. C. M., Lefeber, D. J., Friedl, P., and van Delft, F. L. (2010) *Angew. Chem., Int. Ed. 49*, 9422−5.
(22) Dommerholt, J., van Rooijen, O., Borrmann, A., Guerra, C. F., Bickelhaupt, F. M., and van Delft, F. L. (2014) *Nat. Commun. 5*, 5378.
(23) Debets, M. F., van Berkel, S. S., Schoffelen, S., Rutjes, F. P. J. T., van Hest, J. C. M., and van Delft, F. L. (2010) *Chem. Commun. 46*, 97−9.
(24) Hagendorn, T., and Bräse, S. (2014) *RSC Adv. 4*, 15493.
(25) Hagendorn, T., and Bräse, S. (2014) *Eur. J. Org. Chem. 2014*, 1280−1286.
(26) Gold, B., Dudley, G. B., and Alabugin, I. V. (2013) *J. Am. Chem. Soc. 135*, 1558−69.
(27) Debets, M. F., van Berkel, S. S., Dommerholt, J., Dirks, A. T., Rutjes, F. P., and van Delft, F. L. (2011) *Acc. Chem. Res. 44*, 805−15.
(28) Meldal, M., and Tornøe, C. W. (2008) *Chem. Rev. 108*, 2952−3015.
(29) Becer, C. R., Hoogenboom, R., and Schubert, U. S. (2009) *Angew. Chem., Int. Ed. 48*, 4900−4908.
(30) Hein, J. E., and Fokin, V. V. (2010) *Chem. Soc. Rev. 39*, 1302−15.
(31) Lutz, J. F. (2008) *Angew. Chem., Int. Ed. 47*, 2182−4.
(32) Debets, M. F., van der Doelen, C. W. J., Rutjes, F. P. J. T., and van Delft, F. L. (2010) *ChemBioChem 11*, 1168−1184.
(33) Borrmann, A., and Hest, J. C. M. (2014) *Chem. Sci. 5*, 2123−2134.
(34) Sletten, E. M., and Bertozzi, C. R. (2009) *Angew. Chem., Int. Ed. 48*, 6974−98.
(35) Baumhover, N. J., Martin, M. E., Parameswarappa, S. G., Kloepping, K. C., O'Dorisio, M. S., Pigge, F. C., and Schultz, M. K. (2011) *Bioorg. Med. Chem. Lett. 21*, 5757−61.
(36) Schultz, M. K., Parameswarappa, S. G., and Pigge, F. C. (2010) *Org. Lett. 21*, 2398−2401.
(37) Schobel, U., E, H.-J., Fröhlich, D., Brecht, A., Oelkrug, D., and Gauglitz, D. (2000) *Fluoresc. 2*, 147−154.
(38) Johnson, I., and Spence, M. T. Z. (2010) *The Molecular Probes handbook: A Guide to fluorescent Probes and labeling Technologies*, Life Technologies Corporation, United States.
(39) Atto-Tec; Atto-Tec GmbH, Siegen, Germany, 2013.
(40) *Lifetime Data of Selected Fluorophores*, ISS, http://www.iss.com/resources/reference/data_tables/LifetimeDataFluorophores.html, 2014.
(41) Wurm, C. A., Kolmakov, K., Göttfert, F., Ta, H., Bossi, M., Schill, H., Berning, S., Jakobs, S., Donnert, G., Belov, V. N., and Hell, S. W. (2012) *Optical Nanoscopy 1*, 7.
(42) Schermelleh, L., Heintzmann, R., and Leonhardt, H. (2010) *J. Cell Biol. 190*, 165−75.
(43) Fernandez-Suarez, M., and Ting, A. Y. (2008) *Nat. Rev. Mol. Cell Biol. 9*, 929−43.
(44) Manova, R., van Beek, T. A., and Zuilhof, H. (2011) *Angew. Chem., Int. Ed. 50*, 5428−30.
(45) Wilson, J. T., Krishnamurthy, V. R., Cui, W., Qu, Z., and Chaikof, E. L. (2009) *J. Am. Chem. Soc. 131*, 18228−9.
(46) Frey-Forgues, S., and Lavabre, D. (1999) *J. Chem. Ecol.*, 1260−1264.
(47) Dempsey, G. T., Vaughan, J. C., Chen, K. H., Bates, M., and Zhuang, X. (2001) *Nat. Methods 8* (12), 1027−36.

DOI: 10.1021/acs.bioconjchem.5b00059
Bioconjugate Chem. 2015, 26, 718−724